

# Relativistic many-body calculations of energy levels, hyperfine constants, electric-dipole matrix elements and static polarizabilities for alkali-metal atoms.

M. S. Safronova, W. R. Johnson, and A. Derevianko  
*Department of Physics, Notre Dame University,*  
*Notre Dame, IN 46556*  
 (February 2, 2008)

## Abstract

Removal energies and hyperfine constants of the lowest four  $ns$ ,  $np_{1/2}$  and  $np_{3/2}$  states in Na, K, Rb and Cs are calculated; removal energies of the  $n=7-10$  states and hyperfine constants of the  $n=7$  and 8 states in Fr are also calculated. The calculations are based on the relativistic single-double (SD) approximation in which single and double excitations of Dirac-Hartree-Fock (DHF) wave functions are included to all-orders in perturbation theory. Using SD wave functions, accurate values of removal energies, electric-dipole matrix elements and static polarizabilities are obtained, however, SD wave functions give poor values of magnetic-dipole hyperfine constants for heavy atoms. To obtain accurate values of hyperfine constants for heavy atoms, we include triple excitations partially in the wave functions. The present calculations provide the basis for reevaluating PNC amplitudes in Cs and Fr.

31.15.Ar, 31.25.Jf, 32.10.Fn, 32.10.Dk, 32.70.Cs

## I. INTRODUCTION

Energy levels, transition matrix elements, hyperfine constants, and static polarizabilities for low-lying  $s_{1/2}$ ,  $p_{1/2}$  and  $p_{3/2}$  states in alkali-metal atoms are studied systematically using the relativistic single-double (SD) method in which single and double excitations of the Dirac-Hartree-Fock (DHF) wave function are included to all orders of perturbation theory. The SD method was applied previously to study properties of Li and  $\text{Be}^+$  [1], Li, Na, and Cs [2], Cs [3], and Na-like ions with  $Z$  ranging from 11 to 16 [4]. In the latter study, the theoretical removal energies for Na-like ions, when corrected for the Lamb shift, agreed with experiment at the  $1\text{--}20\text{ cm}^{-1}$  level of accuracy for all states considered, while theoretical hyperfine constants and dipole matrix elements typically agreed with precise measurements to better than 0.3%.

Energies of alkali-metal atoms have been calculated to high precision in [5] using the relativistic coupled-cluster (CC) method; however, there have been no systematic CC studies of hyperfine constants or transition amplitudes for alkali-metal atoms. All-order methods are needed for such studies since correlation corrections are large in alkalis and low-order many-body perturbation theory (MBPT) does not give accurate results for atomic properties. In K, Rb, and Cs, third-order MBPT gives ground state energies in poorer agreement with experiment than second-order MBPT, as illustrated in Table I where zeroth-order DHF energies are tabulated together with second- and third-order MBPT corrections. The differences  $\Delta^{(k)}$ ,  $k = 0, 2, 3$  between experimental energies and accumulated MBPT values shown in Table I oscillate above and below the experimental values and show no sign of convergence. In the SD approximation, an important subset of MBPT diagrams is iterated to all orders in perturbation theory, leading to energies in excellent agreement with experiment.

During the last few years, lifetimes of the lowest  $p_{1/2}$  and  $p_{3/2}$  levels have been measured to high precision for all alkali-metal atoms [6–12], yielding experimental dipole matrix elements accurate to 0.1%–0.25%. In the present work, electric-dipole matrix elements for  $n'p - ns$  transitions in alkalis from Na to Fr are evaluated for  $n = N, N + 1$  and  $n' = N, \dots, N + 3$ , where  $N$  is the principle quantum number of the ground state. Matrix elements and energies from the present SD calculation were used in Ref. [13] to study polarizabilities of alkali-metal atoms.

In this paper, we discuss our calculation of static polarizabilities in detail and show that the *ab-initio* SD results are in excellent agreement with the values recommended in [13]. We also calculate Stark-induced scalar and vector transition polarizabilities for  $Ns - (N + 1)s$  transitions. The accuracy of our calculations is discussed and recommended values of scalar and vector polarizabilities are provided for Cs and Fr. These values are needed for the interpretation of experiments on parity nonconservation in atoms [14].

A systematic study of hyperfine constants for  $s$ ,  $p_{1/2}$  and  $p_{3/2}$  levels is also presented. The accuracy of SD calculations of hyperfine constants for alkali-metal atoms decreases rapidly from 0.3% for Na to 7% for Cs. To obtain more accurate values for heavy alkalis, it was found necessary to include triple excitations to the wave functions partially. The derivation of an approximate single-double partial triple (SDpT) wave function is given in the following section.

In summary, we study low-lying  $s$  and  $p$  levels in alkali-metal atoms in the relativistic SD and SDpT approximations and find excellent agreement with other high-precision cal-

culations and with available experimental data. The SDpT wave functions from the present calculations will be used later to evaluate parity nonconserving (PNC) amplitudes in cesium and francium.

## II. TRIPLE EXCITATIONS

The all-order single-double method was described previously in Refs. [1–4]. Briefly, we represent the wave function  $\Psi_v$  of a one valence electron atom as  $\Psi_v \approx \Psi_v^{\text{SD}}$  with

$$\begin{aligned} \Psi_v^{\text{SD}} = & \left[ 1 + \sum_{ma} \rho_{ma} a_m^\dagger a_a + \frac{1}{2} \sum_{mnab} \rho_{mnab} a_m^\dagger a_n^\dagger a_b a_a \right. \\ & \left. + \sum_{m \neq v} \rho_{mv} a_m^\dagger a_v + \sum_{mna} \rho_{mnva} a_m^\dagger a_n^\dagger a_a a_v \right] \Phi_v, \end{aligned} \quad (1)$$

where  $\Phi_v$  is the lowest-order atomic state function, which is taken to be the *frozen-core* DHF wave function of a state  $v$ . In this equation,  $a_i^\dagger$  and  $a_i$  are creation and annihilation operators, respectively, for state  $i$ . Indices at the beginning of the alphabet,  $a, b, \dots$ , refer to occupied core states, those in the middle of the alphabet  $m, n, \dots$ , refer to excited states, and  $v$  refers to valence orbital. Substituting the wave function (1) into the many-body Schrödinger equation, where the Hamiltonian is taken to be the relativistic *no-pair* Hamiltonian with Coulomb interactions [15], one obtains the coupled equations for single- and double-excitation coefficients  $\rho_{mv}$ ,  $\rho_{ma}$ ,  $\rho_{mnva}$ , and  $\rho_{mnab}$ . The coupled equations are solved iteratively for the excitation coefficients. We use the resulting SD wave functions to evaluate hyperfine constants and electric-dipole matrix elements. It was shown in [4] that the SD energies are not complete in third order and that the missing third-order energy contributions are associated with the omitted triple-excitations. In [4], we calculated the missing third-order terms separately and added them to the final energies. It can be shown that one-body matrix elements calculated using SD wave functions are complete through third order. As mentioned in the introduction, hyperfine constants for heavy alkali-metal atoms are not determined to high precision in the SD approximation. However, by adding the two triple-excitation terms  $\rho_{mnrvab}$  and  $\rho_{mnrab}$  to the SD wave function, we automatically include the missing third-order energy and also substantially improve the accuracy of our calculations of hyperfine constants. The corrected wave function is

$$\begin{aligned} \Psi_v \approx \Psi_v^{\text{SD}} + & \left[ \frac{1}{6} \sum_{mnrab} \rho_{mnrvab} a_m^\dagger a_n^\dagger a_r^\dagger a_b a_a a_v \right. \\ & \left. + \frac{1}{18} \sum_{mnrab} \rho_{mnrab} a_m^\dagger a_n^\dagger a_r^\dagger a_c a_b a_a \right] \Phi_v, \end{aligned} \quad (2)$$

where  $\Psi_v^{\text{SD}}$  is single-double wave function in Eq. (1). The addition of the core term  $\rho_{mnrab}$  is necessary to preserve the symmetry relation  $\rho_{mnva} = \rho_{nmav}$ . Carrying out the calculations, we obtain the following equations for the energy, single- and double-excitation coefficients:

$$\delta E_v = (\text{SD}) + \sum_{mnab} g_{abmn} \rho_{mnrvab}, \quad (3)$$

$$(\varepsilon_a - \varepsilon_m) \rho_{ma} = (\text{SD}) + \sum_{nrbc} g_{bcnr} \rho_{mnrbac} , \quad (4)$$

$$(\varepsilon_v - \varepsilon_m + \delta E_v) \rho_{mv} = (\text{SD}) + \sum_{nrab} g_{abnr} \rho_{mnrvab} , \quad (5)$$

$$\begin{aligned} (\varepsilon_a + \varepsilon_b - \varepsilon_m - \varepsilon_n) \rho_{mnab} = & (\text{SD}) \\ & - \sum_{rcd} g_{cdar} \rho_{mnrbdc} - \sum_{rcd} g_{cdbr} \rho_{nmradc} - \sum_{rsc} g_{cmrs} \rho_{snrbac} - \sum_{rsc} g_{cnrs} \rho_{smrabc} , \end{aligned} \quad (6)$$

$$\begin{aligned} (\varepsilon_a + \varepsilon_v - \varepsilon_m - \varepsilon_n + \delta E_v) \rho_{mnva} = & (\text{SD}) \\ & + \sum_{rcb} g_{bcar} \rho_{mnrvcb} + \sum_{rc} g_{bcvr} \rho_{mnrbac} + \sum_{rsb} g_{bmrs} \rho_{srnvba} + \sum_{rsb} g_{bnrs} \rho_{srnvab} . \end{aligned} \quad (7)$$

In the above equations, we write out only those terms arising from the triple excitations. The quantities  $\varepsilon_i$  are single-particle energies and  $\delta E_v$  is the correlation correction to the valence energy. Below, we use the notations  $\varepsilon_{mn} = \varepsilon_m + \varepsilon_n$ ,  $\tilde{g}_{abcd} = g_{abcd} - g_{abdc}$  and  $\tilde{\rho}_{abcd} = \rho_{abcd} - \rho_{abdc}$ . The contributions from the single- and double-excitation coefficients, designated by (SD) above, are given in Ref. [4]. We require that the triple-excitation coefficients  $\rho_{mnrvab}$  and  $\rho_{mnrbac}$  be antisymmetric with respect to any non-cyclic permutation of the indices  $mnr$ ,  $vab$  and  $mnr$ ,  $abc$ , respectively, and we obtain the following equations for the triple-excitation coefficients:

$$\begin{aligned} (\varepsilon_a + \varepsilon_b + \varepsilon_c - \varepsilon_m - \varepsilon_n - \varepsilon_r) \rho_{mnrbac} = \\ \sum_{\substack{123 = \{mnr\} \\ 1'2'3' = \{abc\}}} \frac{1}{2} \left( \frac{1}{2} g_{121'2'} \rho_{33'} - \sum_d g_{1d1'2'} \rho_{23d3'} + \sum_s g_{23s3'} \rho_{1s1'2'} \right) + [\text{triples}] , \end{aligned} \quad (8)$$

$$\begin{aligned} (\varepsilon_a + \varepsilon_b + \varepsilon_v - \varepsilon_m - \varepsilon_n - \varepsilon_r + \delta E_v) \rho_{mnrvab} = \\ \sum_{\substack{123 = \{mnr\} \\ 1'2'3' = \{vab\}}} \frac{1}{2} \left( \frac{1}{2} g_{121'2'} \rho_{33'} - \sum_c g_{1c1'2'} \rho_{23c3'} + \sum_s g_{23s3'} \rho_{1s1'2'} \right) + [\text{triples}] , \end{aligned} \quad (9)$$

where [triples] groups together terms containing  $\rho_{mnrvab}$  or  $\rho_{mnrbac}$ . In the above equations, the notation  $123 = \{mnr\}$  designates symbolically that the indices 123 range over all six permutations of the indices  $mnr$ ; even permutations contribute with a positive sign while odd permutations contribute with a negative sign. The relatively small contributions from single- and triple-excitations on the right-hand sides of Eqs. (8) and (9) are omitted in the present study.

The dominant triples corrections arise from the triple contributions to  $\delta E_v$  and  $\rho_{mv}$  given in Eq. (3) and Eq. (5), respectively. Solving the equation for  $\rho_{mnrvab}$  and substituting the resulting expression into Eq. (3), we find

$$\begin{aligned} \delta E_v \approx & (\text{SD}) + \sum_{mnab} \frac{\tilde{g}_{abmn}}{\varepsilon_{ab} - \varepsilon_{mn}} \left\{ \sum_c \tilde{g}_{cmav} \tilde{\rho}_{nvbc} + \sum_s \tilde{g}_{nv as} \tilde{\rho}_{msvb} + \sum_c \tilde{g}_{cvbv} \rho_{mnca} \right. \\ & \left. + \sum_s \tilde{g}_{mvsv} \rho_{nsba} + \sum_c g_{cmab} \tilde{\rho}_{vnvc} + \sum_s g_{mnas} \tilde{\rho}_{vsbv} + \sum_s g_{mnvs} \rho_{vsba} + \sum_c g_{cvba} \rho_{mnvc} \right\} . \end{aligned} \quad (10)$$

Repeating these steps for  $\rho_{mv}$ , we obtain from Eq. (5):

$$\begin{aligned}
(\varepsilon_v - \varepsilon_m + \delta E_v) \rho_{mv} \approx (\text{SD}) - \sum_{nrab} \frac{\tilde{g}_{abnr}}{(\varepsilon_{ab} - \varepsilon_{nr})} \left\{ \sum_c \tilde{g}_{ncva} \tilde{\rho}_{rmcb} - \sum_s \tilde{g}_{rmsa} \tilde{\rho}_{snvb} + \sum_c \tilde{g}_{mcva} \rho_{nrcb} \right. \\
\left. - \sum_s \tilde{g}_{rmsv} \rho_{nsab} + \sum_c g_{ncab} \tilde{\rho}_{rmcv} - \sum_s g_{nrsv} \tilde{\rho}_{smvb} - \sum_s g_{nrsv} \rho_{msab} + \sum_c g_{mcab} \rho_{nrcv} \right\}. \quad (11)
\end{aligned}$$

In our numerical studies, we use the approximation

$$\frac{\tilde{g}_{abmn}}{\varepsilon_{ab} - \varepsilon_{mn}} \approx \tilde{\rho}_{mnab}$$

in Eqs. (10) and (11). In the present calculations, we include triples in the  $\rho_{mv}$  and  $\delta E_v$  equations only. As discussed above, only double-excitation terms are considered in the equations for the triple-excitation coefficients. Finally, *explicit* triple-excitation corrections to matrix elements are omitted; only indirect corrections caused by modification of  $\delta E_v$  and  $\rho_{mv}$  are included. The modified matrix elements are evaluated as described in Ref. [4]. In the approximation used here, all third-order corrections to  $\delta E_v$  are automatically included.

### III. RESULTS AND DISCUSSIONS

#### A. Removal energies and fine structure

The SD equations are set up in a finite basis and solved iteratively to give the single- and double-excitation coefficients  $\rho_{ma}$ ,  $\rho_{mv}$ ,  $\rho_{mnab}$  and  $\rho_{mnva}$ , and the correlation energy  $\delta E_v$ . The basis orbitals used to define the single-particle states are linear combinations of B-splines [16]. For each angular momentum state, the basis set consisted of 40 basis orbitals constructed from 40 B-splines of order 7. In our iterative calculations, we used only 35 of the 40 orbitals. The B-spline basis orbitals were interpolated onto a 250 point nonlinear radial grid. All orbitals were constrained to a large spherical cavity; the cavity radii were chosen to be 110 a.u. for Na, 100 a.u. for K and Rb, 75 a.u. for Cs, and 90 a.u. for Fr. Such large cavities were needed to accommodate the highly excited states considered here. The DHF energies of the lowest 3-4  $s$  and  $p$  states were reproduced to five or more significant digits by the B-spline basis functions. Generally, the larger values of  $n$  had lower accuracy, which is unimportant owing to the decreasing size of correlation corrections with increasing  $n$ . Terms in the angular-momentum decomposition with angular momentum  $l$  from 0 to 6 were retained in the basis and the partial-wave contributions were extrapolated to give the final values of the correlation energy. The extrapolation procedure is described in [4]. For the case of Fr, only partial waves with  $l \leq 5$  were retained because of computational limitations, and the extrapolation procedure was simplified, leading to somewhat lower accuracy.

Contributions to the energy from the Breit interaction (with all-order correlation corrections) were obtained as expectation values of the Breit operator using SD wave functions, as described in [4]. Breit corrections were found to be less than  $15\text{cm}^{-1}$  in all cases.

In Fig. 1, values of  $\delta E_v$  for the ground states of the alkalis, corrected for missing triples, are compared with the second-order energy  $E^{(2)}$ , the third-order energy  $E^{(2)}+E^{(3)}$ , and with the experimental correlation energy  $E_{\text{expt}}$ . Differences between  $\delta E_v$  and  $E^{(2)}+E^{(3)}$  are from fourth- and higher-order terms in the MBPT expansion. It is clear from the figure that the

SD procedure resolves the problem of poor convergence of MBPT discussed previously and shown in Table I, and that the SD ground-state correlation energies are in good agreement with experimental values. Contributions from fourth- and higher-order corrections increase from 8% of the total correlation energy for Na to 24% for Fr. Differences with measurements for the ground-state correlation energy range from 0.1% for Na to 2.7% for Fr. The SD approximation, therefore, accounts for a dominant fraction of the fourth- and higher-order correlation energy. Correlation corrections for lowest  $p_{1/2}$  states are about 3 times smaller than those for the ground states. The relative contributions of higher-order corrections are found to be approximately the same for  $ns$  and  $np$  states.

A detailed comparison of removal energies for  $s$  and  $p_{1/2}$  states with experiment is given in Table II. The experimental data used in this comparison are from Ref. [17] except for Fr, where experimental energies compiled in [18] and results of recent measurements [19] are used. For Na, our theoretical uncertainty (from extrapolation) ranges from  $0.4 \text{ cm}^{-1}$  for the  $3s$  state to  $0.04 \text{ cm}^{-1}$  for the  $6s$  state; this uncertainty increases for heavier alkalis. The agreement with experiment is excellent for Na, where the  $6s$  energy differs from experiment by  $0.14 \text{ cm}^{-1}$  and the  $3s$  energy differs by  $2 \text{ cm}^{-1}$ . The corresponding differences are 5–48  $\text{cm}^{-1}$  in K, 7–42  $\text{cm}^{-1}$  in Rb, 17–145  $\text{cm}^{-1}$  in Cs, and 16–114  $\text{cm}^{-1}$  in Fr. Agreement with experiment improves substantially with  $n$  since correlation corrections decrease. Our results for removal energies of  $np_{1/2}$  states are in excellent agreement with experiment for all states considered. For  $np_{1/2}$  states, differences with experiment are  $0.1\text{--}0.6 \text{ cm}^{-1}$  in Na,  $2\text{--}4 \text{ cm}^{-1}$  in K,  $1\text{--}7 \text{ cm}^{-1}$  in Rb,  $9\text{--}24 \text{ cm}^{-1}$  in Cs, and  $13\text{--}29 \text{ cm}^{-1}$  in Fr. The removal energies of  $np$  states are expected to be in better agreement with experiment because of the smaller size of correlation corrections. We make predictions of  $9p_{1/2}$  and  $10p_{1/2}$  energies in Fr (where there are no experimental values) in the last row of Table II. These predictions are based on the comparison of SD energies with experimental energies for other  $np$  states in Cs and Fr. We expect our predictions to be accurate to about  $5 \text{ cm}^{-1}$ . Experimental energies for all states, except the  $np$  states of Na, are larger than theoretical values; in other words, correlation corrections are generally underestimated in the SD approximation.

The SD energies are compared with the relativistic CC calculations from Ref. [5] and with MBPT calculations from [18] in Table III. The CC calculations agree better with experiment for  $ns$  states except for the case of Na, where the CC energy differs from experiment by about  $100 \text{ cm}^{-1}$  for the  $3s$  ground state. For the  $np$  states, the present calculations are in better agreement with experiment than the CC calculations, especially for the  $6p_{1/2}$  state of Rb, and the  $7p_{1/2}$  state of Cs.

The fine-structure intervals  $np_{3/2} - np_{1/2}$  are compared with experiment and with relativistic CC calculations [5] in Table IV. Predictions for the fine-structure intervals of the  $8p$  and  $9p$  states in Fr, based on comparisons of other intervals in Cs and Fr, are also given in the table. The theoretical fine-structure intervals are seen to be in uniformly excellent agreement with experiment.

In summary, the relativistic SD approximation gives accurate values for  $ns$  removal energies in alkali-metal atoms, the agreement with experiment being better for lighter elements. Removal energies for  $np$  states and  $np_{3/2} - np_{1/2}$  fine-structure intervals are also in excellent agreement with experiment.

## B. Electric-dipole matrix elements

Electric-dipole matrix elements for  $n'p_{1/2} - ns$  and  $n'p_{3/2} - ns$  transitions are evaluated in the SD approximation using the formalism laid out in [1]. In brief, the one-particle matrix element  $Z$  is represented in second quantization as

$$Z = \sum_{ij} z_{ij} a_i^\dagger a_j, \quad (12)$$

where  $z_{ij}$  is the matrix element of the dipole operator  $z$  between single-particle orbitals. In the SD approximation, matrix elements of  $Z$  are obtained by substituting SD wave function from Eq. (1) into the matrix element  $\langle \Psi_w | Z | \Psi_v \rangle$ . Correcting for normalization, one obtains:

$$\langle \Psi_w^{\text{SD}} | Z | \Psi_v^{\text{SD}} \rangle = \delta_{wv} Z_{\text{core}} + \frac{Z_{\text{val}}^{\text{SD}}}{[(1 + \delta N_w^{\text{SD}})(1 + \delta N_v^{\text{SD}})]^{1/2}}, \quad (13)$$

where the first term contributes for scalar operators only. The term  $Z_{\text{val}}^{\text{SD}}$  is the sum

$$Z_{\text{val}}^{\text{SD}} = z_{wv} + z_{wv}^{(a)} + \cdots + z_{wv}^{(t)}, \quad (14)$$

where  $z_{wv}$  is the DHF matrix element and the remaining 20 terms are linear or quadratic functions of the single- and double-excitation coefficients  $\rho_{ma}$ ,  $\rho_{mv}$ ,  $\rho_{mnab}$  and  $\rho_{mnva}$ . Expressions for the terms  $z_{wv}^{(i)}$  and the normalization constant  $\delta N_v^{\text{SD}}$  are given in Ref. [1].

Matrix elements for  $n'p_{1/2} - ns$  and  $n'p_{3/2} - ns$  transitions with  $n' = N \cdots N + 3$  and  $n = N, N + 1$ , where  $N$  is the principal quantum number of the ground state, are calculated using this method. The resulting matrix elements are subsequently used to evaluate polarizabilities. In Fr, electric-dipole matrix elements of  $n'p - 9s$  transitions are also calculated to provide additional data for this least studied alkali-metal atom.

In Table V, we compare SD matrix elements for the principal  $Np_{1/2} - Ns$  and  $Np_{3/2} - Ns$  transitions in Na, K, Rb, Cs, and Fr with the high-precision experimental results from [7,9,12]. The differences between the present SD calculations and experiment range from 0.1% in Na to 0.5–0.8% in Fr. The SD results for the principal transitions are in all cases in better agreement with experiments than the third-order MBPT values from [20] because of the more complete treatment of higher-order corrections. In Cs, which has been extensively studied during the past fifteen years, all-order results from Refs. [21] and [22] are also available. Comparison of our results with these theoretical calculations will be given below. Reduced matrix elements for transitions from all  $n'p_{1/2}$  and  $n'p_{3/2}$  states to  $Ns$  and  $(N + 1)s$  states of Na, K, and Rb are given in Table VI. These matrix elements are used later to evaluate polarizabilities. Except for the principal transitions, no high-precision experimental values are available for these matrix elements.

It is possible to include effects of triple excitations indirectly by using valence single- and double-excitation coefficients  $\rho_{mv}$  and  $\rho_{mnva}$  modified as explained previously to include triples partially. Equation (14) itself is not modified in this procedure, thus, effects of the triples are included only indirectly. We use this procedure to obtain SDpT values for hyperfine constants. We found that including triples indirectly does not improve the agreement with experiment for matrix elements of principal transitions, except for Na; for transitions other than the principal ones the accuracy improves slightly.

To improve the accuracy of the matrix elements further, one must include triple excitations *explicitly* in the matrix elements, i.e. calculate matrix elements in Eq. (14) using the SDT wave function given in Eq. (2). As a result, expressions for  $Z_{\text{val}}$  will be modified:

$$Z_{\text{val}}^{\text{SDT}} = Z_{\text{val}}^{\text{SD}} + [\text{triples}], \quad (15)$$

where [triples] are terms containing triple excitation coefficients  $\rho_{mnrvab}$  and  $\rho_{mnrabc}$ .

It is possible to estimate the contribution of some omitted higher-order terms. The dominant correlation corrections to most of the transition matrix elements are from the Brueckner-orbital (BO) terms defined in [4] and discussed in Refs. [3] and [20]. To estimate the effect of omitted higher-order corrections to the BO terms, we scaled the single-excitation coefficients  $\rho_{mv}$ , as described in Ref. [21]: the coefficients were multiplied by the ratios of the experimental to theoretical correlation energies. In Table VII, scaled results for Cs matrix elements are compared with our SD data, with the all-order calculations of Refs. [21,22], and with experiment. The experimental data for  $6p - 6s$  transitions in this table are from the most recent measurement [12]. For the other transitions, with the exception of  $7p - 7s$ , the experimental data compiled in Ref. [22] are used. Matrix elements for  $7p_{1/2} - 7s$  and  $7p_{3/2} - 7s$  transitions can be determined accurately from a recent high-precision measurement of the Stark shift [23]. Values determined in this way (described more completely in the following section) are listed instead of experimental data for these two transitions since no accurate experimental values are available. We also list matrix elements from Ref. [24], where experimental and theoretical data were compiled to provide “best values”. As we can see from the Table VII our *ab-initio* SD calculations provide accurate values for all of the matrix elements with the exception of  $np - 6s$ . For  $np - 6s$  transitions, omitted higher-order corrections are very large, but can be estimated using the scaling procedure described above. Results from Refs. [21] and [22] were obtained using similar scaling procedures, however, the relative importance of scaling is different in each case owing to the different treatment of correlation corrections. In Ref. [21], scaling gave small (0.2-0.4%) contributions for all transitions [3], while in Ref. [22] scaling led to 5.5% and 4% changes in  $7p_{1/2} - 6s$  and  $7p_{3/2} - 6s$  matrix elements and 0.1% to 0.7% changes in the others. For our SD calculations, scaling changes matrix elements for  $7p_{1/2} - 6s$  and  $7p_{3/2} - 6s$  transitions by 6% and 4% respectively, and results for all other transitions by 0.5-1.2%. Our scaled matrix elements in Cs are in excellent agreement with other accurate theoretical results and with experimental values for transitions other than the principal transition. For the principal transition, the present scaled values are in poorer agreement with experiment, since scaling does not account for missing fourth- and higher-order RPA terms [4] that contribute significantly in this case. For other transitions, scaling of the SD results substantially increases the accuracy, allowing us to make reasonable predictions for the corresponding transitions in Fr where no experimental results are available, and to estimate the accuracy of Fr polarizability calculations.

In Table VIII, we compare our results for  $n's - np_{1/2}$  and  $n's - np_{3/2}$ , matrix elements in francium with theoretical calculations from Refs. [18,20,25], and with experiment [9]. As for other alkali-metal atoms, the present all-order results agree better with experiment than the MBPT results from Ref. [20]. The results from the all-order calculations of [18] are shown in column (a) of Table VIII and the predictions from [18] are shown in column (b). Our SD results for the  $8s - 7p$  transitions are between the values shown in columns (a) and (b), while SD data for  $8s - 8p$  transitions are very close to values from (b). The only transition



for which there is a large discrepancy between the SD values and those from Ref. [18] is  $7s - 8p_{1/2}$ . As previously noted, there is a large contribution to this matrix element from triple excitations that can be estimated by scaling. The scaled SD matrix element for this transition, listed in second column of Table VIII is in much better agreement with Ref. [18]; it differs by 5% from the result (a) and by 2% from the prediction (b). This transition is particularly hard to calculate since the total correlation correction is about 40% (about twice as large as for the  $7s - 7p_{1/2}$  transition), and a more accurate treatment of higher-order corrections is required. Our SD result for the  $7s - 8p_{3/2}$  transition agrees with Ref. [18] to 1%. Recently, a large number of  $n'p - ns$  matrix elements in Fr were evaluated using a semi-empirical model potential method [25]. These semi-empirical values agree with the *ab-initio* SD calculations to better than 1% with the exceptions of the  $7s - 8p$  and  $7s - 9p$  transitions, where contributions from correlation corrections are very large. The scaled SD data, which are more accurate for these four transitions, are in good agreement with [25].

In conclusion, the all-order SD method gives accurate data for a wide range of  $n'p - ns$  matrix elements for all alkali-metal atoms with exception of some transitions, such as  $7s - 8p$  in Fr, which have small dipole matrix elements and large correlation corrections. The accuracy for such transitions is significantly improved by scaling single excitation coefficients. To achieve higher precision for electric-dipole matrix elements and to improve the accuracy of other matrix elements in Cs and Fr, a more complete treatment of triple excitations is necessary.

### C. Static polarizabilities

As mentioned in the introduction, SD matrix elements and energies were used to calculate static polarizabilities, Van der Walls coefficients, and atom-wall interaction coefficients of alkali-metal atoms in [13]. We discuss the calculation of the static polarizabilities in more detail here. The polarizabilities of the ground states of alkali-metal atoms are given by the sum of two terms,  $\alpha = \alpha_v + \alpha_a$  where  $\alpha_v$  is the contribution from valence excited states and  $\alpha_a$  is the contribution from core excited (autoionizing) states. The contribution of the autoionizing states can be well approximated by  $\alpha_c$ , the polarizability of the ionic core. We write  $\alpha_a = \alpha_c + \alpha_{vc}$ , where  $\alpha_{vc}$  is a counter term compensating for Pauli-principle violating excitations from the core to the valence shell. For an alkali atom in its  $Ns$  ground state, these contributions are given by,

$$\alpha_v = \frac{1}{3} \sum_{n'} \left( \frac{|\langle Ns || z || n'p_{1/2} \rangle|^2}{E_{n'p_{1/2}} - E_{Ns}} + \frac{|\langle Ns || z || n'p_{3/2} \rangle|^2}{E_{n'p_{3/2}} - E_{Ns}} \right), \quad (16)$$

$$\alpha_c = \frac{2}{3} \sum_{ma} \frac{|\langle a || z || m \rangle|^2}{E_m - E_a}, \quad (17)$$

$$\alpha_{vc} = \frac{1}{3} \sum_a \frac{|\langle a || z || Ns \rangle|^2}{E_a - E_{Ns}}. \quad (18)$$

The expressions for  $\alpha_c$  and  $\alpha_{vc}$  above are written in the single-particle approximation.

The dominant term is the valence contribution  $\alpha_v$ . This term is evaluated by summing over the first few values of  $n'$  in Eq. (16) explicitly and approximating the remainder. Thus,  $\alpha_v = \alpha_v^{\text{main}} + \alpha_v^{\text{tail}}$ . In the term  $\alpha_v^{\text{main}}$ , we included  $n'p$  states with  $n'=3-7$  for Na,  $n'=4-7$  for

K,  $n'=5-8$  for Rb,  $n'=6-9$  for Cs; and  $n'=7-10$  for Fr. All matrix elements were calculated using SD wave functions. These states account for more than 99% of  $\alpha_v$ ; the small remainder  $\alpha_v^{\text{tail}}$  was evaluated in the DHF approximation and is expected to be accurate to better than 15% for Na and 50% for Fr. The core polarizability  $\alpha_c$  which contributes less than 10% of the total in all cases was calculated using the relativistic random-phase approximation (RRPA). Values of  $\alpha_c$  for  $\text{Na}^+$ ,  $\text{K}^+$ ,  $\text{Rb}^+$ , and  $\text{Cs}^+$  were taken from Ref. [26] and the RRPA value for  $\text{Fr}^+$  was obtained in a separate calculation [13]. The resulting values of  $\alpha_c$  are expected to be accurate to better than 5% based on comparisons with recommended values from Miller and Bederson [27]. The much smaller valence-core contributions  $\alpha_{vc}$  were evaluated using DHF wave functions.

A breakdown of contributions to ground-state polarizabilities is given in Table IX, together with a comparison with recommended values from [13] and experiment [28–30]. In this table and in the paragraphs below, values of the polarizabilities are given in atomic units ( $a_0^3$ ). The SD results for Na, K, Rb, and Cs are in excellent agreement with the values recommended in Ref. [13] which were obtained using high-precision experimental matrix elements for the principal transitions and experimental energies. In the case of Fr, the difference is 1%; however, the accuracy of the recommended value is 0.75%. The difference in Fr is in part due to the lower accuracy of the SD dipole matrix elements for the principal transition compared to the accuracy of these matrix elements for other alkalis.

Stark-induced scalar and vector polarizabilities  $\alpha_S$  and  $\beta_S$  for transitions from  $Ns$  to the  $(N+1)s$  states were also calculated. The vector polarizability  $\beta_S$  is important for the interpretation of PNC experiments [14]. In addition, we evaluated differences  $\Delta\alpha$  between polarizabilities of the  $(N+1)s$  states and the  $Ns$  ground states. Formulas for  $\alpha_S$  and  $\beta_S$  are given in [21]. Cesium is the only alkali-metal atom for which experimental data are available for all three of these parameters. The present calculations provide useful reference data for the lighter alkali-metal atoms and for Fr.

Contributions to  $\alpha_S$  and  $\beta_S$  are listed in Table X together with comparisons with experiment and with semi-empirical calculations from Ref. [24]. The core contributions vanish for the Stark polarizabilities but the core-valence contributions  $\alpha_{vc}$  and  $\beta_{vc}$  do not. The terms  $\alpha_S^{\text{tail}}$ ,  $\alpha_{vc}$ ,  $\beta_S^{\text{tail}}$  and  $\beta_{vc}$  were evaluated in the DHF approximation, which is sufficient since these terms give small fractions of the totals. The data in the rows labeled  $\alpha_S^{SD}$  and  $\beta_S^{SD}$  were obtained using SD data for energies and matrix elements. The SD value for the scalar transition polarizability  $\alpha_S$  in Cs differs from the experimental value by 1.5%. As we see from Table X,  $\beta_S$  is very small for Na but increase rapidly with  $Z$ . Our value of 26.87 for Cs is in good agreement with the latest experimental value  $\beta_S = 27.024(43)_{\text{expt}}(67)_{\text{theory}}$  from Ref. [31]. The vector polarizability  $\beta_S$  is especially difficult to calculate precisely, since  $np_{1/2}$  and  $np_{3/2}$  terms contribute with opposite sign. For example, the  $6p_{1/2}$  contribution is -154.90 and the  $6p_{3/2}$  contribution is 171.74. As a result, even small uncertainties in the values of matrix elements can lead to large errors. The principal uncertainties in  $\beta_S$  are from  $7s-6p$  and  $7p-6s$  matrix elements. It should be noted that it is sufficient to accurately know the ratio of  $(np_{3/2} - n's)/(np_{1/2} - n's)$  matrix elements to significantly reduce the error.

To estimate the accuracy of the SD value and to provide recommended values for scalar and vector transition polarizabilities in Cs and Fr we also calculate  $\alpha_S$  and  $\beta_S$  using experimental energies and matrix elements for the principal transitions and scaled SD matrix elements for the other transitions listed in Table VII. This semi-empirical calculation leads

to the recommended values in Table X with the exception of the value of  $\beta_S$  in Cs, which is listed in the separate row. The accuracy of the value of  $\alpha_S$  is calculated assuming independent uncertainties in all matrix elements, where the uncertainties are based on the comparisons with experiment. The main contribution to the error in  $\alpha_S$  comes from uncertainties in the  $7p_{3/2} - 6s$  matrix element, which is accurate to 2%. The contribution of other uncertainties is insignificant. The resulting value of  $\alpha_S$  is in excellent agreement with the experimental value. To estimate the accuracy of vector transition polarizability, we calculate  $\beta_S$  using our recommended value of  $\alpha_S$  and the high-precision experimental ratio  $\alpha_S/\beta_S=9.905(11)$  [32]. The resulting value of  $\beta_S$ , which is listed as the recommended value of Table X is 27.11(22) with error coming dominantly from the calculation of  $\alpha_S$ . As we see, this value is consistent with our direct calculation of  $\beta_S=27.16$ . Further improvement in the accuracy of values of scalar and vector polarizability will be possible when an accurate experimental value of the  $7p_{3/2} - 7s$  matrix element is obtained. Our recommended values of  $\alpha_S$  and  $\beta_S$  in Cs are in excellent agreement with values obtained by Dzuba, Flambaum, and Sushkov [24]. Uncertainties in the values of  $\alpha_S$  and  $\beta_S$  in Ref. [24] are lower than the uncertainties of our recommended values owing to the fact that a 0.7% uncertainty to the experimental value of  $7p_{3/2} - 6s$  matrix element is assigned in Ref. [24].

We also carried out calculations of  $\alpha_S$  and  $\beta_S$  in Fr using both methods described above. The results from the rows labeled “Recomm.” are obtained by using experimental values of energies and principal transition matrix elements together with scaled SD data from Table VIII. The SD results  $\alpha_S^{SD}$  and  $\beta_S^{SD}$  agree with our recommended values within 0.8% for  $\alpha_S$  and 1.4%  $\beta_S$ . As in the case of Cs, the uncertainty in the value of  $\alpha_S$  is dominated by assuming that errors in all the transitions are independent. The uncertainties are obtained by the uncertainty of the  $8p_{3/2} - 7s$  matrix element, which is 2% based on comparison with Cs data. The final uncertainty in  $\alpha_S$  in Fr is 1%; the uncertainty in  $\beta_S$  is also 1% based on a comparison with Cs.

Table XI gives the contribution to  $\Delta\alpha$ , the difference between the static polarizabilities of the  $(N + 1)s$  states and the  $Ns$  ground states of alkali-metal atoms. The SD value  $\Delta\alpha^{SD}$  of the scalar transition polarizability for Cs differs from the recent experimental result 5837(6) [23] by 0.4% and agrees within the error limits with the theoretical result 5833(80) from Ref. [21]. As noted previously, the experimental value of  $\Delta\alpha$  can be used to derive  $7p - 7s$  matrix elements to high accuracy, since  $\Delta\alpha$  depends almost entirely on the values of these matrix elements. The values of  $7p_{1/2} - 7s$  and  $7p_{3/2} - 7s$  matrix elements were varied to yield experimental value of  $\Delta\alpha$  within experimental precision. Ratio of these matrix elements  $D(7p_{3/2} - 7s)/D(7p_{1/2} - 7s)$  is taken to be 1.3892(3) based on the theoretical calculations. Experimental data were used for  $6s - 6p$ ,  $6s - 7p$ , and  $7s - 6p$  matrix elements and theoretical values were used for all others. The results are  $D(7p_{1/2} - 7s)=10.308(5)$  and  $D(7p_{3/2} - 7s)=14.320(7)$  assuming uncertainty only in the experimental value of  $\Delta\alpha$ . The only other significant uncertainty is from the 0.5% error in the value of  $6p - 7s$  matrix elements (which results in a 0.1% variation in the value of  $\Delta\alpha$ ). The final results, accounting for the uncertainties in all matrix elements and in the experimental value of  $\Delta\alpha$ , are  $D(7p_{1/2} - 7s)=10.308(15)$  and  $D(7p_{3/2} - 7s)=14.320(20)$ . We give a recommended value for  $\Delta\alpha$  in Fr obtained in the same way as recommended value for  $\alpha_S$ . The uncertainty in this value comes almost entirely from the uncertainty in the  $8p - 8s$  matrix elements, which is taken to be 0.3%.

## D. Hyperfine Constants

Results of our calculations of magnetic-dipole hyperfine constants  $A$  (MHz) for  $ns$ ,  $np_{1/2}$  and  $np_{3/2}$  states in Na, K, Rb and Cs are given in Table XII together with experimental values from [33–37]. The nuclear magnetic moments used in the calculations are weighted averages of values taken from the tabulation by Raghavan [38]; they are listed in Table XIII. The calculations include corrections for the finite size of the nuclear magnetic moment distribution, which is modeled as a uniformly magnetized ball. The magnetization radii  $R_m$  are obtained using nuclear parameters given in Ref. [39] and are also listed in Table XIII. The rows labeled DHF in Table XII give results calculated in the lowest-order DHF approximation. The all-order results, including triple contributions as described in section II, are listed in the rows labeled SDpT. As stated in the introduction, the SD method gives poor results for ground-state hyperfine constants in alkalis, except for Na. In fact, the SD result for the  $6s$  hyperfine constant in Cs, without corrections for triples, overestimates the experimental value by 7%, which is worse than the corresponding third-order MBPT result. As can be seen, the SDpT values are generally in excellent agreement with experiment for  $ns$  and  $np_{1/2}$  states. For the ground state of Cs, the agreement with experiment improves to 1% using SDpT wave functions. Differences between SDpT results and experiment are greater than 1% for  $np_{3/2}$  states of Rb and Cs. Further improvements of the accuracy of the hyperfine constants will require a more complete treatment of triples.

In the calculations described above, corrections due to the finite size of the nuclear magnetic moment distribution (FS) in Na, K, and Rb are very small and are included in zeroth-order only. However, FS corrections to hyperfine constants are significant for Cs and Fr and are, therefore, included to all orders. The relative size of the FS contributions to the correlation correction in  $ns$  states in these cases is found to be the same as in the lowest-order DHF calculation. Breit corrections to the hyperfine constants are calculated in second order following the method outlined in [40]. These corrections are negligible for Na and K, but grow rapidly from 0.1% for  $5s$  state of Rb to 0.5% for the  $7s$  state of Fr.

The SDpT values of hyperfine constants  $A$  for the  $7s$ ,  $7p_{1/2}$ ,  $7p_{3/2}$ ,  $8s$ ,  $8p_{1/2}$ , and  $8p_{3/2}$  states in  $^{211}\text{Fr}$  are given in Table XIV, where comparisons are made with experimental [19,41,42] and other theoretical data [43]. It should be noted that FS corrections contribute 2.5% to the  $7s$  hyperfine constant. The values of  $7s$  and  $7p_{1/2}$  hyperfine constants for  $^{211}\text{Fr}$  differ from experimental values by 1.4% and 1.8%, respectively; however, the accuracy of the magnetic moment  $\mu = 4.00(8) \mu_N$  [41] is 2%. It should be noted that the SDpT result for the  $6s$  state of Cs underestimates the experimental hyperfine constant by 1% but the SDpT result for the  $7s$  state of Fr overestimates the experiment value by 1.4%. The relative contribution of correlation for the Fr  $7s$  hyperfine constant is about the same as for the Cs  $6s$  hyperfine constant. Possible reasons for the anomalous differences with experiment are uncertainties in the Fr magnetic moment or magnetic moment distribution; a more precise value of the magnetic moment is required to draw conclusions about the accuracy of the correlation correction. The value of  $A$  for the  $7p_{3/2}$  state in Fr differs from experiment by 3.2%; however, it is lower than the experimental value, unlike values for  $7s$  and  $7p_{1/2}$  states. The main source of theoretical uncertainty for the  $7p_{3/2}$  hyperfine constant is the correlation correction, as it is for the Cs  $6p_{3/2}$  hyperfine constant. Our results are in good agreement with theoretical calculation of [43], where the Fr hyperfine constants were calculated using

MBPT. It should be noted that our results include Breit correction and a more complete treatment of the correlation and, thus, are expected to provide more accurate results for Fr hyperfine constants.

The dependence of the FS correction on the value of magnetization radius was investigated in lowest order. Values of  $A(7s)$  for Fr obtained with magnetization radii  $R_m=6.5$  fm and  $R_m=7.0$  fm but with the same charge radius  $C_{nuc}=6.71$  fm differ by 0.2%. The  $7s$  hyperfine constants calculated with  $C_{nuc}=R_m=6.5$  fm and  $C_{nuc}=R_m=7.0$  fm differ by 0.5% of the total value.

## E. Conclusion

We have presented a systematic study of properties of alkali-metal atoms using relativistic single-double wave functions. These wave functions give accurate values of removal energies, fine-structure intervals, electric-dipole matrix elements, and polarizabilities for alkali-metal atoms from Na to Fr. The SD wave functions, however, lead to hyperfine constants for heavier alkali-metal atoms that differ substantially from precise measurements. To obtain accurate values for hyperfine constants, it was necessary to include triples (partially) in the wave function. This was done using the SDpT wave functions described in Section II and leads to accurate values of hyperfine constants. Energies and transition matrix elements in Na determined here agree with those from the earlier SD calculation of Ref. [4]; similarly, the present energies and matrix elements in Cs are in close agreement with the SD calculations of Ref. [21]. The SD calculations for K, Rb, and Fr presented here are completely new.

The theoretical SD ground-state removal energies differ from experiment by amounts ranging from  $2\text{ cm}^{-1}$  in Na to  $114\text{ cm}^{-1}$  in Fr, and the SD removal energies for  $np$  states agree with experimental values better than  $30\text{ cm}^{-1}$  for all states considered. The theoretical SD matrix elements for principal transitions agree with recent high-precision experiments to 0.1-0.5%, with exception of the  $7s - 7p_{3/2}$  transition in Fr where the difference is 0.8%. The agreement with experiment is better for lighter systems because of the smaller size of the correlation corrections. A large number of matrix elements, which were used to calculate polarizabilities, are tabulated for all alkali metal atoms; these matrix elements should provide useful reference data. The SD approximation gives excellent results for static polarizabilities and for Stark-induced transition polarizabilities. Supplementing our theoretical calculations with experimental energies and experimental matrix elements for the two principal transitions, allowed us to predict values of the Stark polarizabilities  $\alpha_S$  and  $\beta_S$  for in Cs and Fr to high accuracy. The predicted values for  $\alpha_S$  and  $\beta_S$  in Cs are in excellent agreement with experimental values. Hyperfine constants, calculated using SDpT wave functions, are in excellent agreement with experiment for  $ns$  and  $np_{1/2}$  states of alkali-metal atoms from Na to Cs. Differences between theoretical SDpT ground-state hyperfine constants and experiment ranges from 0.3% in Na to 1.4% in Fr. The contributions of Breit and FS corrections to the ground state hyperfine constant in Fr are found to be significant. A more precise experimental value for the Fr nuclear magnetic moment is necessary to evaluate the accuracy of correlation corrections to Fr hyperfine constants.

The methods developed in this work will be used in the future to evaluate PNC amplitudes in Cs and Fr.

## ACKNOWLEDGMENTS

This work was supported in part by National Science Foundation Grants Nos. PHY-95-13179 and PHY-99-70666.

## REFERENCES

- [1] S.A. Blundell, W.R. Johnson, Z.W. Liu, and J. Sapirstein, Phys. Rev. A **40**, 2233 (1989).
- [2] Z.W. Liu, Ph. D. thesis, Notre Dame University, (1989).
- [3] S.A. Blundell, W.R. Johnson, and J. Sapirstein, Phys. Rev. A **43**, 3497 (1991).
- [4] M.S. Safronova, A. Derevianko, and W.R. Johnson, Phys. Rev. A **58**, 1016 (1998).
- [5] E. Eliav, U. Kaldor, and Y. Ishikawa, Phys. Rev. A **50**, 1121 (1994).
- [6] K.M. Jones, P.S. Julienne, P.D. Lett, W.D. Phillips, E. Tiesinga, and C.J. Williams, Europhys. Lett. **35**, 85 (1996).
- [7] U. Volz and H. Schmoranz, Phys. Scr. T **65**, 48 (1996).
- [8] H. Wang, P.L. Gould, W.C. Stwalley, J. Chem. Phys. **106**, 7899 (1997).
- [9] J.E. Simsarian, L.A. Orozco, G.D. Sprouse, and W.Z. Zhao, Phys. Rev. A **57**, 2448 (1998).
- [10] R.J. Rafac, C.E. Tanner, A.E. Livingston, K.W. Kukla, H.G. Berry, and C.A. Kurtz, Phys. Rev. A **50**, 1976 (1994).
- [11] L. Young, W.T. Hill III, S.J. Sibener, S.D. Price, C.E. Tanner, C.E. Wieman, and S.R. Leone, Phys. Rev. A **50**, 2174 (1994).
- [12] R.J. Rafac, C.E. Tanner, A.E. Livingston, and H.G. Berry, Phys. Rev. A (submitted for publication 1998).
- [13] A. Derevianko, W.R. Johnson, M.S. Safronova, and J.F. Babb, Phys. Rev. Lett. **82**, 3589 (1999).
- [14] C. S. Wood, S. C. Bennett, D. Cho, B. P. Masterson, J. L. Roberts, C. E. Tanner, and C. E. Wieman, Science, **275**, 1759 (1997).
- [15] G.E. Brown and D.G. Ravenhall, Proc. R. Soc. London, Ser. A **208**, 552 (1951).
- [16] W.R. Johnson, S.A. Blundell, and J. Sapirstein, Phys. Rev. A **37**, 2764 (1988).
- [17] C.E. Moore, *Atomic Energy Levels*, Natl. Bur. Stand. Ref. Data Ser., Natl. Bur. Stand. (U.S.) Circ. No. 35 (U.S. GPO, Washington, D.C., 1971), Vols. I-III.
- [18] V.A. Dzuba, V.V. Flambaum, and O.P. Sushkov, Phys. Rev. A **51**, 3454 (1995).
- [19] J.E. Simsarian, W. Shi, L.A. Orozco, G.D. Sprouse, W.Z. Zhao, Opt. Lett. **21** (1996), 1939; J.E. Simsarian, W.Z. Zhao, L.A. Orozco, G.D. Sprouse, Phys. Rev. A **59** (1999) 195.
- [20] W.R. Johnson, Z.W. Liu and J. Sapirstein, At. Data and Nucl. Data Tables **64**, 279 (1996); J. Sapirstein, Rev. Mod. Phys. **70**, 55 (1998).
- [21] S.A. Blundell, J. Sapirstein, and W.R. Johnson, Phys. Rev. D **45**, 1602 (1992).
- [22] V.A. Dzuba, V.V. Flambaum, and O.P. Sushkov, Phys. Lett. A **141**, 147 (1989).
- [23] S.C. Bennett, J.L. Roberts, and C.E. Wieman, Phys. Rev. A. **59**, R16 (1999).
- [24] V.A. Dzuba, V.V. Flambaum, and O. P. Sushkov, Phys. Rev. A, **56** 4357 (1997).
- [25] M. Marinescu, D. Vrinceanu, and H.R. Sadeghpour, Phys. Rev. A **58**, R4259 (1998).
- [26] W.R. Johnson, D. Kolb, and K.-N. Huang, At. Data Nucl. Data Tables **28**, 333 (1983).
- [27] T.M. Miller and B. Bederson, Adv. At. Mol. Phys. **13**, 1 (1977).
- [28] C.R. Ekström, J. Schmiedmayer, M.S. Chapman, C.D. Hammond, and D.E. Pritchard, Phys. Rev. A **51**, 3883 (1995).
- [29] R.W. Molof, H.L. Schwartz, T.M. Miller, B. Bederson, Phys. Rev. A **10**, 1131 (1974).
- [30] W.D. Hall and J.C. Zorn, Phys. Rev. A, **10**, 1141 (1974).
- [31] S.C. Bennett and C.E. Wieman, Phys. Rev. Lett **82**, 2484 (1999).

- [32] D. Cho, C.S. Wood, S.C. Bennett, J.L. Roberts, and C.E. Wieman, Phys. Rev. A **55**, 1007 (1997).
- [33] W. Happer in *Atomic Physics 4*, eds. G. zu Putlitz, E.W. Weber, and A. Winnacker, (Plenum Press, New York, 1974) pp. 651-682.
- [34] W.A. Wijngaarden and J. Li, Z. Phys. D **32**, 67 (1994).
- [35] W. Yei, A. Sieradzan and M.D. Havey, Phys. Rev. A **48**, 1909 (1993) .
- [36] R.J. Rafac, C.E. Tanner, Phys. Rev. A **56**, 1027 (1997).
- [37] C.E. Tanner and C. Wieman, Phys. Rev. A **38**, 1616 (1988).
- [38] P. Raghavan, At. Data Nucl. Data Tables **42**, 189 (1989).
- [39] W.R. Johnson and G. Soff, At. Data Nucl. Data Tables **33**, 405 (1985).
- [40] I.M. Savukov, A. Derevianko, H.G. Berry, and W.R. Johnson, submitted to Phys. Rev. Lett.
- [41] C. Ekström, L. Robertsson, A. Rosén, and the ISOLDE collaboration, Phys. Scr. **34**, 624 (1986).
- [42] J.S. Grossman, L.A. Orozco, M.R. Pearson, J.E. Simsarian, G.D. Sprouse, and W.Z. Zhao, submitted to Phys. Rev. Lett.
- [43] V.A. Dzuba, V.V. Flambaum, and O.P. Sushkov, J. Phys. B **17**, 1953 (1984).



# FIGURES

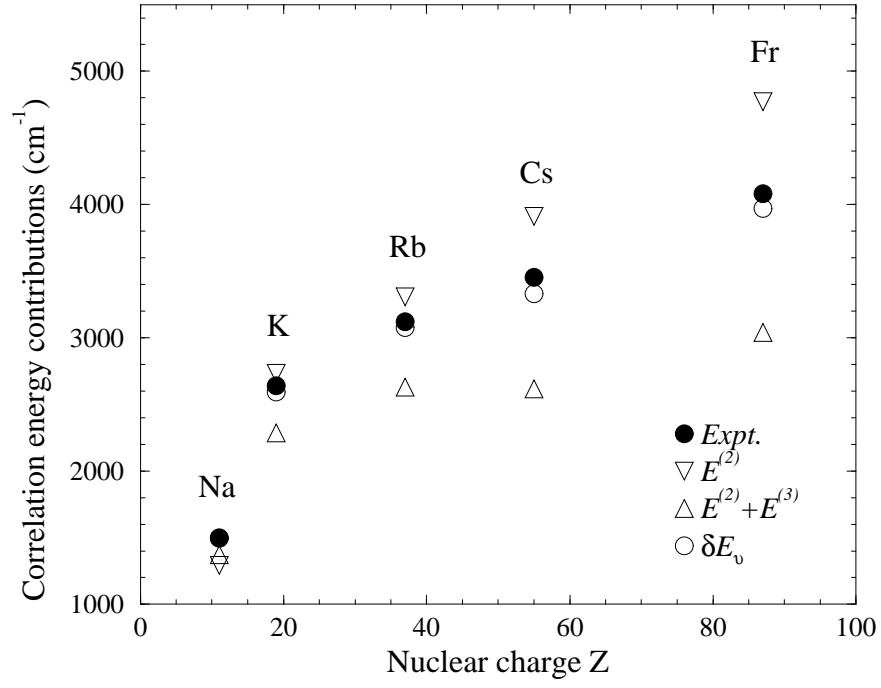


FIG. 1. Comparisons of MBPT and SD correlation corrections to ground state energies for alkali-metal atoms.

# TABLES

TABLE I. Zeroth- (or DHF), second- and third-order MBPT removal energies  $E^{(k)}$  in  $\text{cm}^{-1}$  and energy differences  $\Delta^{(k)} = E_{\text{expt}} - E^{(k)}$ .

$k$	K ( $4s$ )		Rb ( $5s$ )		Cs ( $6s$ )	
	$E^{(k)}$	$\Delta^{(k)}$	$E^{(k)}$	$\Delta^{(k)}$	$E^{(k)}$	$\Delta^{(k)}$
0	32370	2640	30571	3120	27954	3453
2	35104	-94	33878	-187	31865	-458
3	34655	355	33200	491	30529	878
$E_{\text{expt}}$	35010		33691		31407	

TABLE II. Comparison of SD calculations of  $ns$  and  $np_{1/2}$  removal energies with experimental energies from [17–19] in units of  $\text{cm}^{-1}$ .

Na	$3s$	$4s$	$5s$	$6s$
Theory	41447.3	15708.8	8248.48	5076.68
Expt.	41449.4	15709.4	8248.76	5076.82
Na	$3p_{1/2}$	$4p_{1/2}$	$5p_{1/2}$	$6p_{1/2}$
Theory	24493.9	11183.0	6409.31	4153.22
Expt.	24493.3	11182.4	6409.06	4153.12
K	$4s$	$5s$	$6s$	$7s$
Theory	34962	13958	7548	4730
Expt.	35010	13986	7559	4735
K	$4p_{1/2}$	$5p_{1/2}$	$6p_{1/2}$	$7p_{1/2}$
Theory	22023	10304	6008	3938
Expt.	22025	10308	6010	3940
Rb	$5s$	$6s$	$7s$	$8s$
Theory	33649	13527	7365	4637
Expt.	33691	13557	7380	4644
Rb	$5p_{1/2}$	$6p_{1/2}$	$7p_{1/2}$	$8p_{1/2}$
Theory	21111	9969	5852	3854
Expt.	21112	9976	5856	3856
Cs	$6s$	$7s$	$8s$	$9s$
Theory	31262	12801	7060	4479
Expt.	31407	12871	7089	4496
Cs	$6p_{1/2}$	$7p_{1/2}$	$8p_{1/2}$	$9p_{1/2}$
Theory	20204	9621	5687	3760
Expt.	20228	9641	5698	3769
Fr	$7s$	$8s$	$9s$	$10s$
Theory	32735	13051	7148	4522
Expt.	32849	13106	7168	4538
Fr	$7p_{1/2}$	$8p_{1/2}$	$9p_{1/2}$	$10p_{1/2}$
Theory	20583	9712	5724	3782
Expt.	20612	9736	5738 <sup>a</sup>	3795 <sup>a</sup>

<sup>a</sup>Prediction based on SD calculations.

TABLE III. Comparison of SD calculations of  $ns$  and  $np_{1/2}$  removal energies with the CC calculations from Ref. [5] and many-body calculations from Ref. [18] in units of  $\text{cm}^{-1}$ .

Na	$3s$	$4s$	$3p_{1/2}$	$4p_{1/2}$
SD	41447	15709	24494	11183
CC	41352	15690	24465	11172
K	$4s$	$5s$	$4p_{1/2}$	$5p_{1/2}$
SD	34962	13958	22023	10304
CC	35028	13983	22016	10306
Rb	$5s$	$6s$	$5p_{1/2}$	$6p_{1/2}$
SD	33649	13527	21111	9969
CC	33721	13564	21117	9857
Cs	$6s$	$7s$	$6p_{1/2}$	$7p_{1/2}$
SD	31262	12801	20204	9621
CC	31443	12876	20217	9549
Fr	$7s$	$8s$	$7p_{1/2}$	$8p_{1/2}$
SD	32735	13051	20583	9712
CC	32839	13112	20574	9736
[18]	32762	13082	20654	9742

TABLE IV. Comparison of SD fine-structure intervals in Na, K, Rb, Cs, and Fr with experiment and with theoretical CC values from [5]. Units:  $\text{cm}^{-1}$ .

		This work	Expt.	[5]
Na	$3p_{3/2} - 3p_{1/2}$	17.15	17.20	18.35
	$4p_{3/2} - 4p_{1/2}$	5.58	5.63	5.99
	$5p_{3/2} - 5p_{1/2}$	2.46	2.52	
	$6p_{3/2} - 6p_{1/2}$	1.26	1.25	
	$7p_{3/2} - 7p_{1/2}$	0.75	0.74	
K	$4p_{3/2} - 4p_{1/2}$	57.3	57.72	59.45
	$5p_{3/2} - 5p_{1/2}$	18.5	18.8	19.3
	$6p_{3/2} - 6p_{1/2}$	8.5	8.4	
	$7p_{3/2} - 7p_{1/2}$	4.4	4.5	
Rb	$5p_{3/2} - 5p_{1/2}$	236.5	237.6	240.3
	$6p_{3/2} - 6p_{1/2}$	76.5	77.5	87.7
	$7p_{3/2} - 7p_{1/2}$	34.8	35.1	
	$8p_{3/2} - 8p_{1/2}$	18.6	18.9	
Cs	$6p_{3/2} - 6p_{1/2}$	552.2	554.1	554.5
	$7p_{3/2} - 7p_{1/2}$	178.6	181.0	198.4
	$8p_{3/2} - 8p_{1/2}$	81.4	82.6	
	$9p_{3/2} - 9p_{1/2}$	43.9	44.7	
Fr	$7p_{3/2} - 7p_{1/2}$	1676	1687	1670
	$8p_{3/2} - 8p_{1/2}$	536	545	560
	$9p_{3/2} - 9p_{1/2}$	244	250(3) <sup>a</sup>	
	$10p_{3/2} - 10p_{1/2}$	132	136(2) <sup>a</sup>	

<sup>a</sup>Prediction based on SD calculations.

TABLE V. Comparison of SD calculations of reduced dipole matrix elements (a.u.) for the principal transitions in alkali-metal atoms with experimental values.

	Na		K		Rb		Cs		Fr	
	$3p_{1/2} - 3s$	Ref.	$4p_{1/2} - 4s$	Ref.	$5p_{1/2} - 5s$	Ref.	$6p_{1/2} - 6s$	Ref.	$7p_{1/2} - 7s$	Ref.
Present	3.531		4.098		4.221		4.478		4.256	
Expt.	3.5246(23)	[7]	4.102(5)	[7]	4.231(3)	[7]	4.4890(65)	[12]	4.277(8)	[9]
	$3p_{3/2} - 3s$	Ref.	$4p_{3/2} - 4s$	Ref.	$5p_{3/2} - 5s$	Ref.	$6p_{3/2} - 6s$	Ref.	$7p_{3/2} - 7s$	Ref.
Present	4.994		5.794		5.956		6.298		5.851	
Expt.	4.9838(34)	[7]	5.800(8)	[7]	5.977(4)	[7]	6.3238(73)	[12]	5.898(15)	[9]

TABLE VI. SD values of reduced dipole matrix elements (a.u.) in Na, K, and Rb.

Na		K		Rb	
$3p_{1/2} - 3s$	3.531	$4p_{1/2} - 4s$	4.098	$5p_{1/2} - 5s$	4.221
$4p_{1/2} - 3s$	0.305	$5p_{1/2} - 4s$	0.275	$6p_{1/2} - 5s$	0.333
$5p_{1/2} - 3s$	0.107	$6p_{1/2} - 4s$	0.084	$7p_{1/2} - 5s$	0.115
$6p_{1/2} - 3s$	0.056	$7p_{1/2} - 4s$	0.039	$8p_{1/2} - 5s$	0.059
$3p_{1/2} - 4s$	3.575	$4p_{1/2} - 5s$	3.866	$5p_{1/2} - 6s$	4.119
$4p_{1/2} - 4s$	8.376	$5p_{1/2} - 5s$	9.461	$6p_{1/2} - 6s$	9.684
$5p_{1/2} - 4s$	0.943	$6p_{1/2} - 5s$	0.892	$7p_{1/2} - 6s$	0.999
$6p_{1/2} - 4s$	0.377	$7p_{1/2} - 5s$	0.335	$5p_{1/2} - 6s$	0.393
$3p_{3/2} - 3s$	4.994	$4p_{3/2} - 4s$	5.794	$5p_{3/2} - 5s$	5.956
$4p_{3/2} - 3s$	0.435	$5p_{3/2} - 4s$	0.406	$6p_{3/2} - 5s$	0.541
$5p_{3/2} - 3s$	0.154	$6p_{3/2} - 4s$	0.128	$7p_{3/2} - 5s$	0.202
$6p_{3/2} - 3s$	0.081	$7p_{3/2} - 4s$	0.061	$8p_{3/2} - 5s$	0.111
$3p_{3/2} - 4s$	5.066	$4p_{3/2} - 5s$	5.510	$5p_{3/2} - 6s$	6.013
$4p_{3/2} - 4s$	11.840	$5p_{3/2} - 5s$	13.358	$5p_{3/2} - 6s$	13.592
$5p_{3/2} - 4s$	1.341	$6p_{3/2} - 5s$	1.292	$5p_{3/2} - 6s$	1.540
$6p_{3/2} - 4s$	0.537	$7p_{3/2} - 5s$	0.491	$5p_{3/2} - 6s$	0.628

TABLE VII. Comparison of SD reduced dipole matrix elements (a.u.) for Cs with other theoretical values and with experiment.

Transition	SD	scaled	Ref. [21]	Ref. [22]	Expt.	Ref. [24]
$6p_{1/2} - 6s$	4.482	4.535	4.510	4.494	4.4890(65)	
$6p_{3/2} - 6s$	6.304	6.382	6.347	6.325	6.3238(73)	
$7p_{1/2} - 6s$	0.297	0.279	0.280	0.275	0.284(2)	0.2825(21)
$7p_{3/2} - 6s$	0.601	0.576	0.576	0.583	0.583(10)	0.5820(44)
$8p_{1/2} - 6s$	0.091	0.081	0.078			
$8p_{1/2} - 6s$	0.232	0.218	0.214			
$6p_{1/2} - 7s$	4.196	4.243	4.236	4.253	4.233(22)	4.237(22)
$6p_{3/2} - 7s$	6.425	6.479	6.470	6.507	6.479(31)	6.472(31)
$7p_{1/2} - 7s$	10.254	10.310	10.289	10.288	10.308(15) <sup>a</sup>	10.285(31)
$7p_{3/2} - 7s$	14.238	14.323	14.293	14.295	14.320(20) <sup>a</sup>	14.286(43)

<sup>a</sup>Predictions based on the experimental value of the Stark shift [23].

TABLE VIII. Comparison of SD reduced dipole matrix elements (a.u.) for Fr with other theoretical values and with experiment.

	SD	scaled	Ref. [25]	Ref. [18] <sup>a</sup>	Ref. [18] <sup>b</sup>	Ref. [20]	Expt. [9]
$7p_{1/2} - 7s$	4.256			4.279	4.304	4.179	4.277
$8p_{1/2} - 7s$	0.327	0.306	0.304	0.291	0.301		
$9p_{1/2} - 7s$	0.110	0.098	0.096				
$10p_{1/2} - 7s$	0.055						
$7p_{3/2} - 7s$	5.851			5.894	5.927	5.791	5.898
$8p_{3/2} - 7s$	0.934	0.909	0.908	0.924			
$9p_{3/2} - 7s$	0.436	0.422	0.420				
$10p_{3/2} - 7s$	0.271						
$7p_{1/2} - 8s$	4.184	4.237	4.230	4.165	4.219	4.196	
$8p_{1/2} - 8s$	10.02	10.10	10.06	10.16	10.00		
$9p_{1/2} - 8s$	0.985		0.977				
$10p_{1/2} - 8s$	0.380						
$7p_{3/2} - 8s$	7.418	7.461	7.449	7.384	7.470	7.472	
$8p_{3/2} - 8s$	13.23	13.37	13.32	13.45	13.26		
$9p_{3/2} - 8s$	2.245		2.236				
$10p_{3/2} - 8s$	1.049						
$7p_{1/2} - 9s$	1.016		1.010				
$8p_{1/2} - 9s$	9.280		9.342				
$9p_{1/2} - 9s$	17.39		17.40				
$10p_{1/2} - 9s$	1.822						
$7p_{3/2} - 9s$	1.393		1.380				
$8p_{3/2} - 9s$	15.88		15.92				
$9p_{3/2} - 9s$	22.59		22.73				
$10p_{3/2} - 9s$	3.876						

<sup>a</sup>Includes contributions from non-Brueckner diagrams extrapolated from Cs results.

<sup>b</sup>Predictions given in [18].

TABLE IX. Contributions to static polarizabilities (a.u.) of alkali-metal atoms and comparisons with recommended values from [13].

	Na	K	Rb	Cs	Fr
$\alpha_v^{\text{main}}$	162.06	284.70	308.43	383.8	294.0
$\alpha_v^{\text{tail}}$	0.08	0.07	0.14	0.2	1.4
$\alpha_c$	0.95	5.46	9.08	15.8	20.4
$\alpha_{vc}$	-0.02	-0.13	-0.26	-0.5	-0.9
$\alpha^{SD}$	163.07	290.10	317.39	399.3	314.9
Recomm. [13]	162.6(3)	290.2(8)	318.6(6)	399.9(1.9)	317.8(2.4)
Expt.	162.7(8) <sup>a</sup>	293.6(6.1) <sup>b</sup>	319.9(6.1) <sup>b</sup>	403.6(8.1) <sup>b</sup>	

<sup>a</sup>Ref. [28].

<sup>b</sup>Weighted average of experimental data from Refs. [29,30].



TABLE X. Contributions to scalar and vector polarizabilities  $\alpha_S$  and  $\beta_S$  (a.u.) for alkali-metal atoms.

	Na	K	Rb	Cs	Fr
	$3s - 4s$	$4s - 5s$	$5s - 6s$	$6s - 7s$	$7s - 8s$
$\alpha_S^{\text{main}}$	149.66	176.74	235.39	271.00	374.29
$\alpha_S^{\text{tail}}$	0.32	0.28	0.68	0.87	4.22
$\alpha_{vc}$	-0.01	-0.05	-0.11	-0.20	-0.37
$\alpha_S^{SD}$	149.97	176.97	235.96	271.67	378.14
Recomm.				268.6(2.2) <sup>a</sup>	375.3(3.6) <sup>a</sup>
Dzuba <i>et al.</i> [24]				269.0(1.3)	
Expt.				267.6(8) <sup>b</sup>	
$\beta_S^{\text{main}}$	0.35	1.95	9.18	26.77	72.63
$\beta_S^{\text{tail}}$	0.00	0.00	0.04	0.10	0.65
$\beta_{vc}$	0.00	0.00	0.00	0.00	0.01
$\beta_S^{SD}$	0.35	1.95	9.22	26.87	73.29
				27.16 <sup>a</sup>	
Recomm.				27.11(22) <sup>c</sup>	74.3(7) <sup>a</sup>
Dzuba <i>et al.</i> [24]				27.15(13)	
Expt.				27.02(8) <sup>d</sup>	

<sup>a</sup>Values obtained by using experimental values of energies and matrix elements for the principal transitions and scaled SD data for the 8 other transitions listed in Table VII for Cs and Table VIII for Fr.

<sup>b</sup>Value obtained by combining the measurement of  $\beta_S$  [31] with the accurately measured ratio  $\alpha/\beta$  from Ref. [32].

<sup>c</sup>Value obtained by using our recommended value of  $\alpha$  and the experimental  $\alpha/\beta$  ratio from Ref. [32].

<sup>d</sup>Ref. [31].

TABLE XI. Contributions to the differences in static polarizabilities (a.u.) of  $(N+1)s$  and the  $Ns$  ground states of alkali-metal atoms.

	Na	K	Rb	Cs	Fr
$\Delta\alpha^{\text{main}}$	2938.6	4673.7	4851.0	5857.1	4419.5
$\Delta\alpha^{\text{tail}}$	1.9	1.5	2.9	3.0	11.1
$\Delta\alpha_{vc}$	0.0	0.1	0.2	0.4	0.8
$\Delta\alpha^{SD}$	2940.5	4675.3	4854.1	5860.5	4431.4
Recomm.					4517(26) <sup>a</sup>
Expt.				5837(6) <sup>b</sup>	

<sup>a</sup>Value obtained using experimental energies and either experimental or scaled SD matrix elements.

<sup>b</sup>Ref. [23].

TABLE XII. Comparison of SDpT values of hyperfine constants  $A$  (MHz) of  $ns$ ,  $np_{1/2}$ , and  $np_{3/2}$  states of alkali-metal atoms with experiment. Experimental values are from Ref. [33], unless noted otherwise.

Na	$3s$	$4s$	$5s$	$6s$
DHF	623.8	150.5	58.04	28.21
SDpT	888.3	204.3	77.68	37.51
Expt.	885.8	202(3)	78(5)	
Na	$3p_{1/2}$	$4p_{1/2}$	$5p_{1/2}$	$6p_{1/2}$
DHF	63.4	21.0	9.3	4.9
SDpT	95.1	30.7	13.5	7.1
Expt.	94.44(13) <sup>a</sup>			
Na	$3p_{3/2}$	$4p_{3/2}$	$5p_{3/2}$	$6p_{3/2}$
DHF	12.6	4.16	1.85	0.98
SDpT	18.8	6.04	2.66	1.40
Expt.	18.534(15) <sup>b</sup>	6.01(3)		
K	$4s$	$5s$	$6s$	$7s$
DHF	146.8	38.85	15.75	7.89
SDpT	228.6	54.81	21.61	10.68
Expt.	230.85	55.50(60)	21.81(18)	10.85(15)
K	$4p_{1/2}$	$5p_{1/2}$	$6p_{1/2}$	$7p_{1/2}$
DHF	16.61	5.74	2.62	1.41
SDpT	27.65	8.95	4.02	2.14
Expt.	28.85(30)	8.99(15)		
K	$4p_{3/2}$	$5p_{3/2}$	$6p_{3/2}$	$7p_{3/2}$
DHF	3.23	1.11	0.512	0.276
SDpT	5.99	1.93	0.866	0.462
Expt.	6.09(4)	1.97(1)	0.866(8)	
Rb	$5s$	$6s$	$7s$	$8s$
DHF	642.6	171.6	70.3	35.5
SDpT	1011.1	238.2	94.3	46.9
Expt.	1011.9	239.3(1.2)	94.00(64)	45.5(2.0)
Rb	$5p_{1/2}$	$6p_{1/2}$	$7p_{1/2}$	$8p_{1/2}$
DHF	69.8	24.55	11.39	6.19
SDpT	120.4	39.02	17.61	9.45
Expt.	120.7(1)	39.11(3)	17.65(2)	
Rb	$5p_{3/2}$	$6p_{3/2}$	$7p_{3/2}$	$8p_{3/2}$
DHF	12.4	4.37	2.03	1.11
SDpT	24.5	7.98	3.61	1.94
Expt.	25.029(16)	8.25(10)	3.71(1)	
Cs	$6s$	$7s$	$8s$	$9s$
DHF	1425.2	391.6	163.5	83.6
SDpT	2278.5	540.6	217.1	109.1
Expt.	2298.2	545.90(9)	218.9(1.6)	109.5(2.0)

Cs	$6p_{1/2}$	$7p_{1/2}$	$8p_{1/2}$	$9p_{1/2}$
DHF	160.9	57.62	27.08	14.84
SDpT	289.6	93.40	42.43	22.76
Expt.	291.89(8) <sup>c</sup>	94.35	42.97(10)	
Cs	$6p_{3/2}$	$7p_{3/2}$	$8p_{3/2}$	$9p_{3/2}$
DHF	23.93	8.64	4.08	2.24
SDpT	48.51	15.88	7.27	3.93
Expt.	50.275(3) <sup>d</sup>	16.605(6)	7.626(5)	4.129(7)

<sup>a</sup>Ref. [34].

<sup>b</sup>Ref. [35].

<sup>c</sup>Ref. [36].

<sup>d</sup>Ref. [37].

TABLE XIII. Nucleon numbers  $A$ , nuclear spins  $I$ , magnetization radii  $R_m$ (fm) from [39], and magnetic moments  $\mu_I$  in units of  $\mu_N$  from [38] used in the preparation of Table XII.

	$A$	$I$	$R_m$	$\mu_I$
Na	23	3/2	2.89	2.2176
K	39	3/2	3.61	0.39149
Rb	85	5/2	4.87	1.3534
Cs	133	7/2	5.67	2.5826

TABLE XIV. Comparison of SDpT values of Fr hyperfine constants  $A$  (MHz) with experiment and other theory.  $g_I=0.888$ ,  $R_m=6.71$ fm

	$7s$	$7p_{1/2}$	$7p_{3/2}$	$8s$	$8p_{1/2}$	$8p_{3/2}$
DHF	5785.7	622.7	49.30	1482.8	220.91	18.03
SDpT	8833.0	1162.1	91.80	1923.3	362.91	30.41
Expt.	8713.9(8) <sup>a</sup>	1142.0(3) <sup>b</sup>	94.9(3) <sup>a</sup>	1912.5(1.3) <sup>c</sup>		
Ref. [18]	9018	1124	102.2	1970	363.6	35.2

<sup>a</sup>Ref. [41].

<sup>b</sup>Ref. [42].

<sup>c</sup>Value obtained by rescaling experimental value for  $^{210}\text{Fr}$  1577.8(1.1) MHz from Ref. [19] using  $\mu(210)=4.40\mu_N$  and  $\mu(211)=4.00\mu_N$ . The uncertainty includes experimental uncertainty of  $^{210}\text{Fr}$  value 1577.8(1.1) MHz only.